Journal of King Saud University – Computer and Information Sciences 33 (2021) 340–350

Contents lists available at ScienceDirect

Journal of King Saud University – Computer and Information Sciences

journal homepage: www.sciencedirect.com

Polyscale gradients residual demosaicking

M.S. Safna Asiq [a,*], W.R. Sam Emmanuel [b]

[a] Research Scholar, Department of Computer Science, Nesamony Memorial Christian College Affiliated to Manonmaniam Sundaranar University, Thirunelveli, TamilNadu, India
[b] Asso. Prof. Department of P.G. Computer Science, Nesamony Memorial Christian College Affiliated to Manonmaniam Sundaranar University, Thirunelveli, TamilNadu, India

ARTICLE INFO

Article history:
Received 22 December 2017
Revised 5 February 2018
Accepted 28 February 2018
Available online 1 March 2018

Keywords:
Bayer colour filter array
Polyscale gradients
Residual demosaicking

ABSTRACT

Image acquisition through a single-sensor camera captures only a fraction of the image data renowned as the raw image. It uses the colour filter array to acquire only a single colour channel in each pixel location. The reconstruction of the so called raw image into a full colour image is known as demosaicking or interpolation. Demosaicking is a significant process in the imaging pipeline. It implicates the reconstruction of the missing two colour channels from an incomplete image obtained from a single-sensor digital camera. This paper proposes a new approach of combining polyscale gradients algorithm and residual demosaicking. The first phase utilizes the gradients at different scales and residual demosaicking (RD) involves subtraction of the pragmatic and the provisional pixel values in the residual province takes place in the second phase. The experimental results show that the proposed demosaicking algorithm outperforms the conventional demosaicking algorithms for the Kodak and McMaster (McM) dataset.

1. Introduction

The images captured by a single-sensor camera use the Colour Filter Array (CFA). The most commonly used colour filter array is the Bayer colour filter array. In Fig. 1 Bayer (1976) reports a colour imaging array has a combination of luminance and chrominance pixel values. The Bayer CFA consists of green-red and blue-green in the alternate rows, having a maximum number of green channels due to the Human Visual System (HVS) having high sensitivity to green spectrum. It captures only either the red, green or blue pixel values in each pixel location. The restoration of the missing two colour channels in each pixel location is called demosaicking or interpolation. The demosaicking process is initiated by interpolating the green channel followed by the red and blue channels. There are several research works which emphasize the demosaicking algorithms that use Bayer CFA and other CFA patterns.

Demosaicking is based on the spatial and the spectral correlation between the pixels of the image. Buades et al. (2009) has gained self similarity of the image pixel values by obtaining the spectral correlation of the non-local estimate. Chung and Chan (2006) has utilized the variance of colour differences along the edge direction in an edge directed interpolation. Chung et al. (2008) has estimated the gradient adaptively based on the region and edge detection is used to enhance the demosaicking performance, the edge gradient or edge information is extracted directly from the mosaic image based on the spatial and spectral correlation. Duran and Buades (2014) has induced a non-local filtering to the self similarity and spectral correlation of the image pixel values to reduce the chrominance imbalance.

Gunturk et al. (2005) has divided demosaicking into three groups heuristic, restoration problem and generalization using spectral filtering. He et al. (2013) has introduced a guided filter which acts as a smoothing operator to filter the contents of the guidance image. Horé and Ziou (2010) has given an edge detection algorithm to detect the edges in the mosaic image to interpolate the pixel along the edges and not along the edges. Kang et al. (2010) has detected the direction of the edges in the mosaic image based on the spatial correlation of the Bayer colour difference.

Residual interpolation is an alternative to colour difference interpolation. Kiku et al. (2016) has initiated the transformation of the colour difference demosaicking with the residual demosaicking, where the residual demosaicking is the difference between the observed and tentative pixel values. Kiku et al., (2014) has reduced the Laplacian value in residual interpolation which is used to smoothen the image to increase the performance of the demosaicking process. Kiku et al. (2013) has induced the

* Corresponding author at: Research Scholar, Department of Computer Science, Nesamony Memorial Christian College Affiliated to Manonmaniam Sundaranar University, Thirunelveli, TamilNadu, India.
E-mail address: safnabenms@gmail.com (M.S. Safna Asiq).
Peer review under responsibility of King Saud University.

Production and hosting by Elsevier

https://doi.org/10.1016/j.jksuci.2018.02.014
1319-1578/

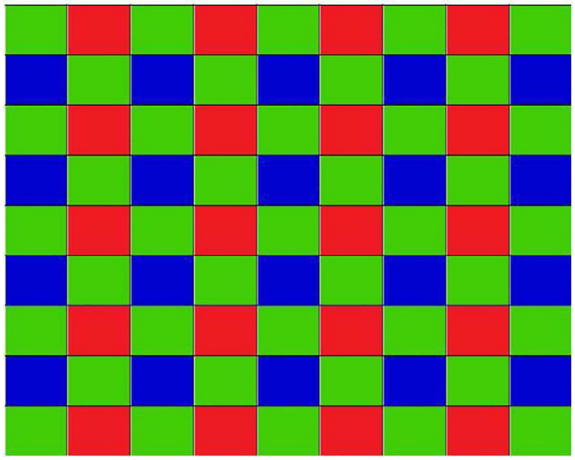

Fig. 1. Bayer Colour Filter Array.

gradient based threshold free algorithm into the residual demosaicking process.

Kim and Jeong (2016) has implemented a four directional residual interpolation combined with a joint inverse gradient weight interpolation. Li et al. (2017) uses the frequency distribution of weights with the threshold value to reduce the artefacts produced at the edges. Lu et al. (2010) portrays a fast one step implementation using alternating projection with high complexity though performance is agreeable. Monno et al. (2015) adaptively selects an iteration number with two residual interpolation algorithms applied at each pixel location. Ousguine et al., (2016) shows that the Laplacian value detects the edge direction for the interpolation process.

The gradients are effective features to extract directional data, Pekkucuksen and Altunbasak (2013) depicts a non-iterative threshold free algorithm in the Bayer and Lukac colour filter array. Pekkucuksen and Altunbasak (2010) implements a gradient based threshold free algorithm to adaptively combine the directional estimates. Wu et al. (2016) in polynomial interpolation predicts the errors and calculates the edges classified by colour difference. Ye and Ma (2015) illustrates an iterative residual interpolation algorithm. Zhang et al. (2016) demonstrates an inter-pixel chrominance capture and optimal demosaicking transformation to skips the luminance components at each pixel location. Zhang et al. (2009) illustrates Linear Minimum Mean Square Error (LMMSE) estimation in the areas of weak or no correlation and a support vector regression to overcome the erroneous areas. Zhang et al. (2005) expiates a directional LMSSE interpolation, Primary Difference Signals (PDS) for optimal directional filtering. Generally, demosaicking has the following application perspectives: it reduces the use of traditional sensors for documenting digital technology of low cost, the tampered images can be identified in forensics, demosaicking produces high dynamic resolution images and segmentation can also be effective through demosaicking.

This proposed novel approach concentrates on the performance and the artefacts in two phases. In the first phase the green channel is interpolated using the colour difference polyscale gradients algorithm and in the second phase, the red and the blue channels are interpolated in the residual province with the guided green image. The residual is the subtraction of the provisional from the pragmatic estimates. The Laplacian value is reduced drastically to increase the smoothness of the image for better demosaicking results. The rest of the paper is illustrated as follows Section 2 describes the background of the proposed work. Section 2.3 explains the proposed work. The experimental results are analyzed with conventional demosaicking algorithms in Sections 3 and Section 4 concludes the paper.

2. Algorithm background

2.1. Polyscale gradients

Pekkucuksen and Altunbasak (2013) replaces the conventional colour difference gradient demosaicking by the Polyscale Gradients (PSG) demosaicking. In the colour difference gradient estimation, the target pixel is two pixels far whereas in polyscale gradients estimation the difference between the colour channels is taken one pixel far from the target pixel at half the scale as in Eq. (1).

$$Dif^{Hor}(a,b) = \left| \frac{Gr(a,b+1) - Gr(a,b-1)}{2} - \frac{(Rd(a,b+2) + Rd(a,b)) - (Rd(a,b-2) + Rd(a,b))}{4} \right|$$
$$Dif^{Ver}(a,b) = \left| \frac{Gr(a+1,b) - Gr(a-1,b)}{2} - \frac{(Rd(a+2,b) + Rd(a,b)) - (Rd(a-2,b) + Rd(a,b))}{4} \right| \quad (1)$$

Where, $Dif^{Hor}(a,b)$ and $Dif^{Ver}(a,b)$ indicates the horizontal and vertical colour difference estimation at half the scale, Gr and Rd indicate the green and red colour channels. The process uses the closest samples, as a good resolution image is obtained with the local colour dynamic in a small scale. The Rd (a, b) cancel out in Eq. (1) at this scale leaving the green and red gradients at twice the scale and further normalized by the distance between the operands.

The direction of the colour channel changes with respect to one another. The horizontal and vertical directional estimates are combined with colour dynamics captured at a more local level and without restoring by simple averaging. The polyscale gradients add additional scales where the locality gets weaker and hence larger scales contributes less to the results. The normalized terms are addressed in the denominator which is the obvious way for optimization. The optimized polyscale gradients equation both horizontally and vertically is illustrated for the red and green rows and columns.

$$Dif^{Hor}(a,b) = \left| \frac{Gr(a,b+1) - Gr(a,b-1)}{2} - \frac{Rd(a,b+2) - Rd(a,b-2)}{Nr_1} + \frac{Gr(a,b+3) - Gr(a,b-3)}{Nr_2} - \frac{Rd(a,b+4) - Rd(a,b-4)}{Nr_3} + \ldots\ldots \right|$$
$$Dif^{Ver}(a,b) = \left| \frac{Gr(a+1,b) - Gr(a-1,b)}{2} - \frac{Rd(a+2,b) - Rd(a-2,b)}{Nr_1} + \frac{Gr(a+3,b) - Gr(a-3,b)}{Nr_2} - \frac{Rd(a+4,b) - Rd(a-4,b)}{Nr_3} + \ldots\ldots \right| \quad (2)$$

Where, Nr_i are the normalized values in varied pixel location based on the size of the image. A 5 × 5 block is applied to the proposed work with the target pixel as the centre pixel and the difference is taken one pixel away from the target pixel. For the blue and green rows and columns, the polyscale gradients equation is the same as the above where the *Rd* pixel values will be replaced by the *Bl* pixel values.

2.2. Residual demosaicking

Prior to the residual demosaicking (RD) the green channel is interpolated first using the polyscale gradients algorithm followed by red and blue channel interpolation by residual demosaicking. The pragmatic estimate of the Rd image is induced from the interpolated Gr image by guided upsampling in which the Laplacian value is minimized. The difference between the pragmatic value and the provisional estimate is known as the residual image. The residual image is then demosaicked and added to the provisionally estimated image to achieve the demosaicked red image.

2.2.1. Guided upsampling

In guided upsampling the provisional estimation is generated using guided filtering (He et al., 2013), it preserves the edges and is independent of the computation time with regard to the size of the filter. Guided upsampling effectively up samples the provisional estimate with respect to the guided green image. The pixel coordinates (i,j) of the provisional image is centred in a local window $\omega_{i,j}$ as

$$\hat{Rd}_{a,b} = P_{i,j}\hat{Gr}_{a,b} + Q_{i,j}, \forall_{a,b} \in \omega_{i,j} \tag{3}$$

Where, $P_{i,j}, Q_{i,j}$ are the linear coefficients simulated as constants. A 5 × 5 window is applied for red and blue channel demosaicking in Section 2.3.3.

2.3. Proposed work

2.3.1. Outline

Kiku et al. (2013) initially applied the Residual Demosaicking (RD) process to restore the missing components from an image obtained from a Bayer colour filter array. The residual demosaicking is the difference between the pragmatic and provisional pixel values in the residual province. The basic processing pipeline of the proposed approach is outlined in Fig. 2. In the first phase, the Gr channel is demosaicked using the colour difference Polyscale Gradients (PSG) algorithm followed by the estimation of the provisional and pragmatic pixel values of Rd channel with Gr as the guided image. The Laplacian value is reduced drastically by guided upsampling for a good demosaicked performance. In the second phase, the residual is demosaicked as a substitute for the traditional colour difference demosaicking. The red and blue channels are demosaicked using residual demosaicking. In the proposed work the residual demosaicking is integrated into the polyscale gradients algorithm.

2.3.2. Green channel interpolation

The Bayer colour filter array consists of a high concentration of green pixel values than the other two colour channels. Like many other demosaicking algorithms the demosaicking process starts with the interpolation of the green channel. Here the polyscale gradients algorithm was used for the green interpolation, where the gradients are the effective features for providing directional data. Fig. 3 pictures the green channel demosaicking using PSG. The directional estimate is identified by the sub-sampled red and green channels as input and the directional colour channel is estimated as the first step of the green channel demosaicking. The green-red channels directional estimates in the horizontal and vertical directions are illustrated in Eq. (4).

$$\begin{aligned}
\hat{Gr}^{Hor}(a,b) &= \frac{Gr(a,b-1)+Gr(a,b+1)}{2} \\
&\quad + \frac{2*Rd(a,b) - Rd(a,b-2) - Rd(a,b+2)}{4} \\
\hat{Gr}^{Ver}(a,b) &= \frac{Gr(a-1,b)+Gr(a+1,b)}{2} \\
&\quad + \frac{2*Rd(a,b) - Rd(a-2,b) - Rd(a+2,b)}{4} \\
\hat{Rd}^{Hor}(a,b) &= \frac{Rd(a,b-1)+Rd(a,b+1)}{2} \\
&\quad + \frac{2*Gr(a,b) - Gr(a,b-2) - Gr(a,b+2)}{4} \\
\hat{Rd}^{Ver}(a,b) &= \frac{Rd(a-1,b)+Rd(a+1,b)}{2} \\
&\quad + \frac{2*Gr(a,b) - Gr(a-2,b) - Gr(a+2,b)}{4}
\end{aligned} \tag{4}$$

vertical directions The colour difference estimate in the horizontal and vertical direction is obtained by finding the difference between the two true colour channels $Gr(a,b), Rd(a,b)$ and the two directional estimates $\hat{Gr}^{Hor}(a,b)$, $\hat{Gr}^{Ver}(a,b)$, $\hat{Rd}^{Hor}(a,b)$ and $\hat{Rd}^{Ver}(a,b)$ for

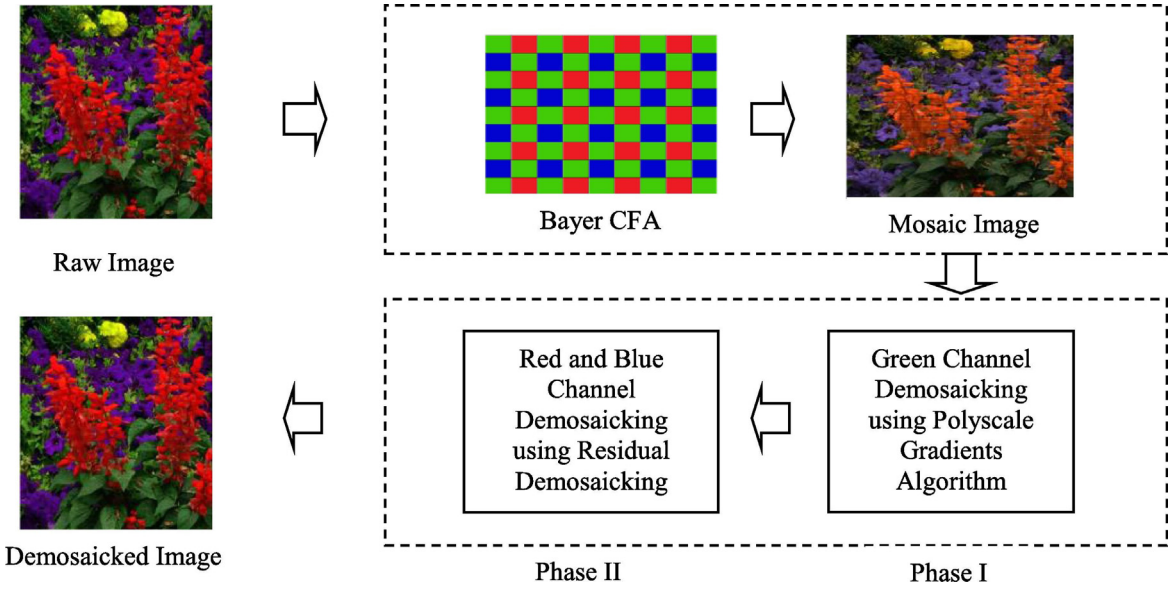

Fig. 2. Block diagram of the proposed work.

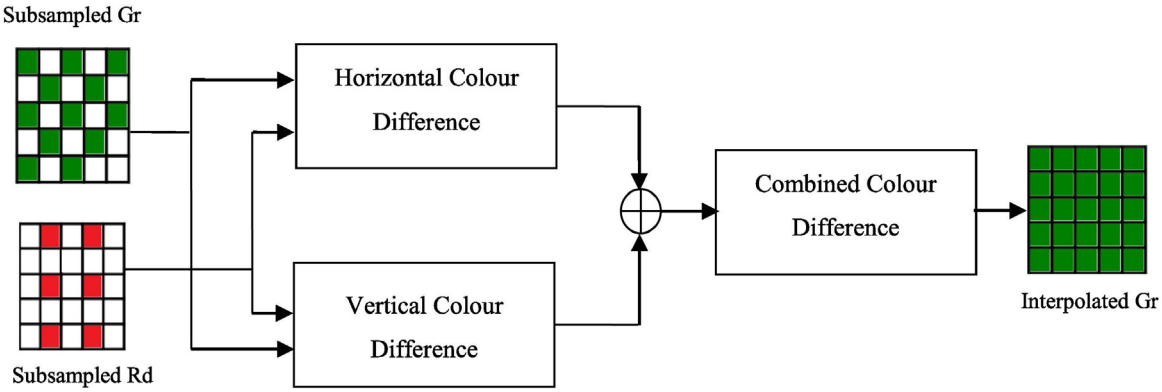

Fig. 3. Structure of the polyscale gradients green interpolation.

pixel each value. The colour difference in the horizontal and vertical directions areas in Eq. (5)

$$\hat{\delta}^{Hor}_{Gr,Rd}(a,b) = \begin{cases} \hat{Gr}^{Hor}(a,b) - Rd(a,b), atGr \\ Gr(a,b) - \hat{Rd}^{Hor}(a,b), atRd \end{cases}$$
$$\hat{\delta}^{Ver}_{Gr,Rd}(a,b) = \begin{cases} \hat{Gr}^{Ver}(a,b) - Rd(a,b), atGr \\ Gr(a,b) - \hat{Rd}^{Ver}(a,b), atRd \end{cases} \quad (5)$$

where, $\hat{\delta}^{Hor}_{Gr,Rd}$ and $\hat{\delta}^{Ver}_{Gr,Rd}$ are the horizontal and vertical colour difference estimates and these colour difference estimates are adaptively combined and smoothed in Eq. (6).

$$\tilde{\delta}_{Gr,Rd}(a,b) = \Big[W_{Ver} * f * \hat{\delta}^{Ver}_{Gr,Rd}(a-1,b) * (a,b) * (a+1,b) + W_{Hor} * \hat{\delta}^{Hor}_{Gr,Rd}(a,b-1) * (a,b) * (a,b+1) * f\Big] / W_{Com}$$
$$W_{Com} = W_{Hor} + W_{Ver} \quad (6)$$

Where, $f = [1/4\ 1/2\ 1/4]$ for a 5 × 5 local window, weight is represented by W in horizontal and vertical directions as W_{Ver}, W_{Hor} and W_{Com} is the constant colour difference assumption. Weight computations for both the directions in a local window as in Eq. (7) for pixel values are evaluated as (c, d) where c = a-2 and d = b-2

$$1/W_{Ver} = \left(\sum_{c=a-2}^{a+2}\sum_{d=b-2}^{b+2} Dif^{Ver}(c,d)\right)^2$$
$$1/W_{Hor} = \left(\sum_{c=a-2}^{a+2}\sum_{d=b-2}^{b+2} Dif^{Hor}(c,d)\right)^2 \quad (7)$$

The green channel is further enhanced to improve the demosaicked result by taking into account of the four adjacent pixel values with their weights (W_N, W_S, W_E, W_W) as in Eq. (8).

$$\hat{\delta}_{Gr,Rd}(a,b) = \tilde{\delta}_{Gr,Rd}(a,b) * (1-W) + [W_N * \tilde{\delta}_{Gr,Rd}(a-2,b) + W_S\tilde{\delta}_{Gr,Rd}(a+2,b) + W_E * \tilde{\delta}_{Gr,Rd}(a,b+2) + W_W * \tilde{\delta}_{Gr,Rd}(a,b-2) * W/W_T$$
$$W_{Tot} = W_N + W_S + W_E + W_W \quad (8)$$

The total weight is denoted as W_{Tot}. The weights are evaluated over a local window of 5 × 3 for vertical channel, as the neighbouring pixel values in the north/south directions are taken into

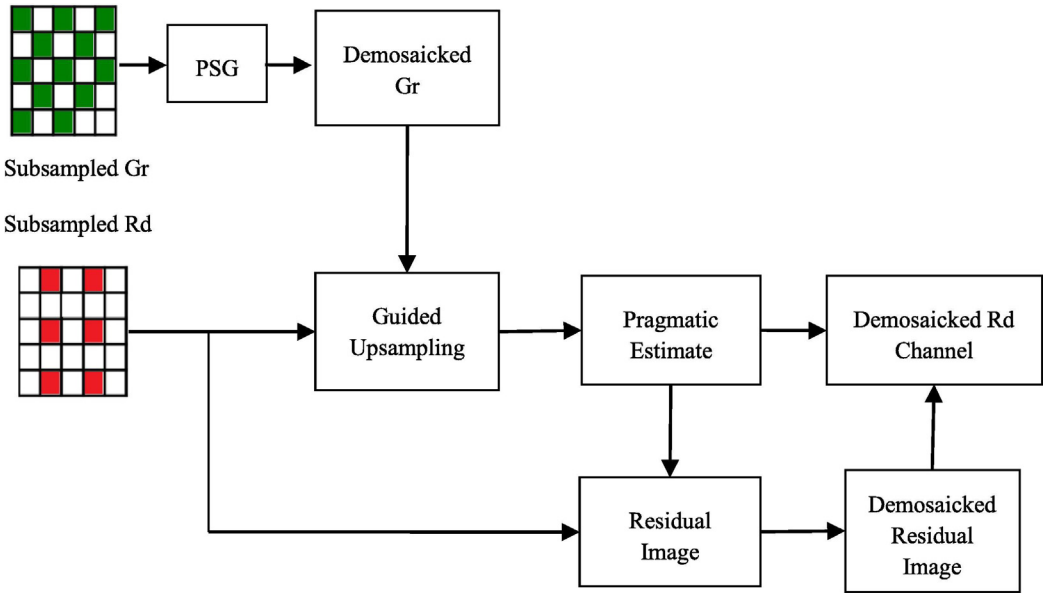

Fig. 4. Outline of Residual demosaicking on red/blue channel.

account from the target pixel in a local area and 3×5 for horizontal channel, as the pixel values in the west/east directions are accounted with respect to the neighbouring pixel values in a local area as explained in Eq. (9). The weight evaluation for four directions North (N), South (S), East (E) and West (W) with its own weights are

$$\begin{aligned} W_N &= 1/\left(\sum_{c=a-4}^{a}\sum_{d=b-1}^{b+1} Dif^{Ver}(c,d)\right)^2 \\ W_S &= 1/\left(\sum_{c=a}^{a+4}\sum_{d=b-1}^{b+1} Dif^{Ver}(c,d)\right)^2 \\ W_E &= 1/\left(\sum_{c=a-1}^{a+1}\sum_{d=b}^{b+4} Dif^{Hor}(c,d)\right)^2 \\ W_W &= 1/\left(\sum_{c=a-1}^{a+1}\sum_{d=b-4}^{b} Dif^{Hor}(c,d)\right)^2 \end{aligned} \tag{9}$$

The weight evaluation for the four adjacent directions is evaluated based on the sum of the difference in horizontal and vertical directions. The estimated green channel is achieved by adding the target pixel and the finally estimated colour difference estimate as in Eq. (10).

$$\begin{aligned} \hat{G}r(a,b) &= Rd(a,b) + \hat{\delta}_{Gr,Rd}(a,b) \\ \hat{G}r(a,b) &= Bl(a,b) + \hat{\delta}_{Gr,Bl}(a,b) \end{aligned} \tag{10}$$

The green channel is demosaicked by adding the provisional Rd and Bl pixel value to the combined colour difference estimate as in Eq. (10). The demosaicked green image now is ready to act as the guide image for the red and blue channel interpolation.

2.3.3. Residual demosaicking on red and blue channels

Residual demosaicking is the latest known demosaicking process. Fig. 4 demonstrates the residual demosaicking process for the red (Rd) channel. The green channel is demosaicked using the PSG algorithm as in Fig. 3. The demosaicked green channel

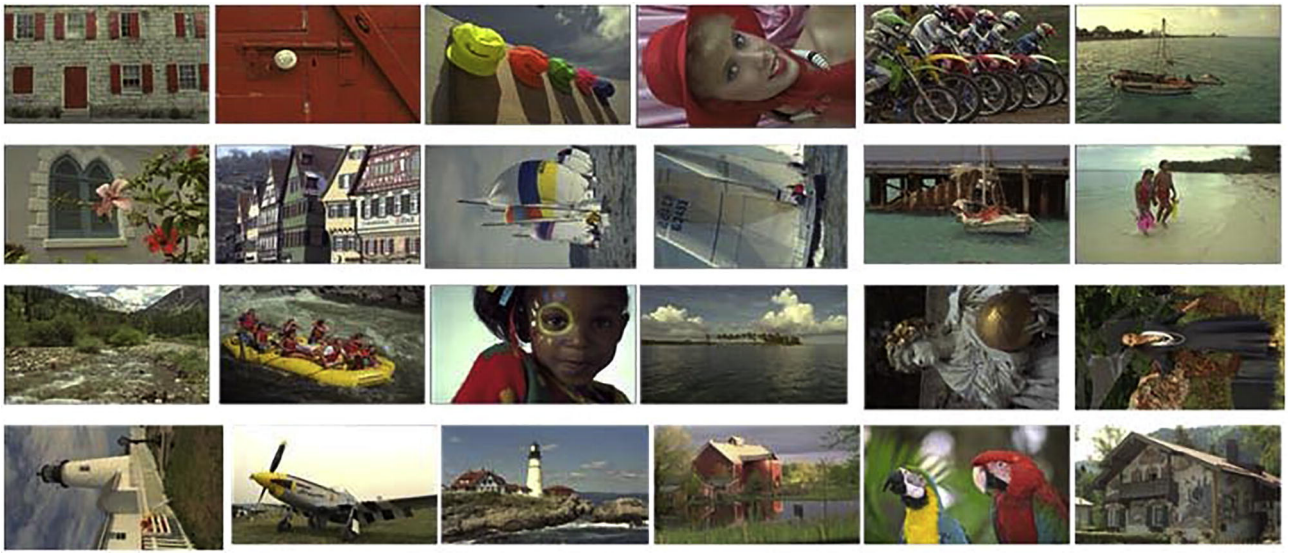

Fig. 5. Test Images of Kodak Dataset.

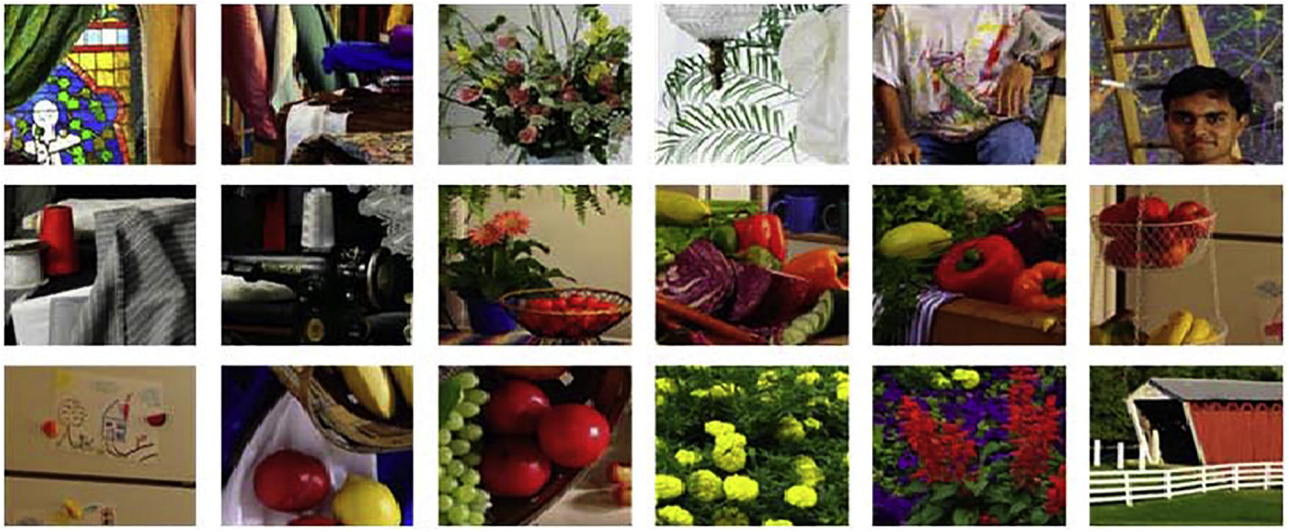

Fig. 6. Test Images of McM Dataset.

Table 1
Comparison of Peak Signal Noise Ratio (PSNR) with conventional demosaicking algorithms for Kodak Dataset.

Image	BI	GBTF	RI	MLRI	MSG	AP	RD-PSG(Prop)
1	26.0440	36.4852	33.8230	34.84366	**36.858**	33.21556	35.96697
2	31.98306	35.2114	28.9276	33.0509	35.559	33.01863	**40.84287**
3	33.01854	37.7854	38.4888	39.3713	38.372	34.44367	**42.77305**
4	32.74294	35.4707	35.6569	36.19512	35.695	33.65322	**40.97679**
5	26.49046	32.226	32.5524	32.95301	32.7414	30.67645	**37.20596**
6	27.41800	37.9766	36.6578	36.99804	38.2640	34.97277	**38.7115**
7	32.46716	36.0264	35.7533	37.0002	36.4462	33.61103	**42.69101**
8	23.55751	33.4547	32.19606	32.8728	33.9563	31.21270	**34.58671**
9	31.77607	39.0395	38.9838	39.7685	39.3488	34.97566	**42.02573**
10	31.66248	38.8861	37.8643	39.0272	39.1526	35.35680	**42.21309**
11	28.94324	36.8343	36.6317	36.7457	37.0617	34.0777	**38.68682**
12	32.21989	39.2248	34.3253	40.3815	39.2665	35.2753	**42.89094**
13	23.87621	34.2043	32.3137	32.9893	**34.5128**	32.5631	32.22369
14	28.77192	30.9766	32.7697	32.69203	31.3054	29.4689	**37.35040**
15	30.76031	36.5413	34.45604	37.5923	36.6243	33.6686	**39.7403**
16	30.56987	41.6965	40.9984	41.3072	42.0878	37.0646	**42.51195**
17	31.37960	40.2403	39.7168	39.9705	**40.626**	35.5975	40.60644
18	27.68512	34.4994	34.4637	34.9174	34.7549	32.7331	**35.96732**
19	27.69540	38.6016	38.1053	37.8993	39.0310	33.3206	**39.4608**
20	30.23682	38.4062	35.0688	38.7018	38.7552	32.5578	**39.9412**
21	28.15376	37.2234	35.9043	36.3387	37.5218	33.5758	**37.53806**
22	29.96614	35.7707	35.6563	36.4083	35.9691	32.8976	**38.13926**
23	34.06215	37.0877	37.0968	38.3961	37.7113	33.2961	**43.10746**
24	26.23973	34.7801	34.1936	34.4577	**35.1018**	31.4911	34.4477
Avg.	29.4883	36.6103	35.5251	36.7032	36.9467	33.4468	39.1919

Table 2
Comparison of PSNR value with conventional demosaicking algorithms using McMaster Dataset.

Image	BI	GBTF	RI	MLRI	MSG	AP	RD-PSG(Prop)
1	25.147	25.1431	27.4644	27.4049	25.4645	23.3603	**29.3059**
2	28.6575	32.5086	33.9669	33.9410	32.7977	30.1277	**35.3379**
3	23.9933	31.2010	31.6487	31.8802	31.5741	29.0024	**33.8628**
4	22.9822	31.2318	34.2898	33.9988	31.9625	27.9228	**37.9826**
5	28.0143	28.5083	31.5689	31.2236	28.6952	27.0434	**34.0930**
6	29.9154	28.7903	33.4163	32.8744	29.0052	27.4125	**38.6527**
7	29.2941	39.9753	38.3126	38.8034	**40.3883**	36.0101	37.0645
8	28.0735	36.2850	35.1743	35.7406	36.5043	33.4668	**37.9663**
9	28.2042	31.1623	33.1703	33.0598	31.5246	29.0370	**36.6068**
10	30.6912	33.3432	35.3278	35.7411	33.8261	30.4729	**38.8804**
11	32.5876	34.1687	36.5318	37.2311	34.6065	31.2501	**40.1854**
12	29.0769	34.9896	37.7424	37.5636	35.2662	31.2067	**39.7916**
13	31.0380	36.9461	40.0751	39.8305	37.1428	32.5784	**40.7343**
14	32.4196	36.6599	38.8507	38.8171	37.0333	33.0920	**39.1140**
15	32.2869	35.9225	36.7287	37.8471	36.3573	32.7168	**39.2090**
16	27.3494	27.7832	31.6597	31.5186	27.8517	25.6390	**35.3746**
17	28.4045	25.3061	28.6098	28.0116	25.6296	24.0386	**32.9546**
18	26.2544	32.5884	34.6288	34.4941	32.8449	29.6127	**36.5008**
Avg.	28.5772	32.3618	34.3981	34.4434	32.6930	29.6661	**36.8676**

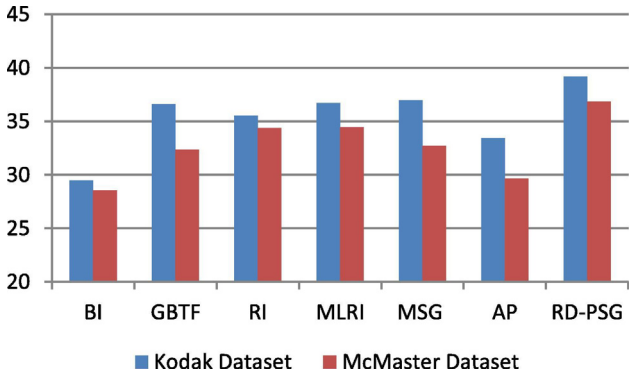

Fig. 7. Comparison of the average PSNR values of the existing and the proposed algorithm.

acts as the guide image and the provisional estimate of the red channel is achieved. The residual image is the difference between the pragmatic and provisional pixel values. As explained in Section 2.2 residual interpolation is performed in a local window $\omega_{i,j}$ with coordinates (i,j). The linear coefficients are $P_{i,j}, Q_{i,j}$ known as the gain and the discriminate component. They are defined as in Eq. (11) to be represented in Eq. (3) of Section 2.2.

$$\hat{P}_{i,j} = \frac{\sum_{i,j\in\omega_{a,b}} W_{i,j}P_{i,j}}{\sum_{a,b\in\omega_{i,j}} W_{i,j}}$$
$$\hat{Q}_{i,j} = \frac{\sum_{i,j\in\omega_{a,b}} W_{i,j}Q_{i,j}}{\sum_{a,b\in\omega_{i,j}} W_{i,j}} \quad (11)$$

Table 3
Comparison of RMSE value with conventional demosaicking algorithms using Kodak Dataset.

Image	BI	GBTF	RI	MLRI	MSG	AP	RD-PSG(Prop)
1	22.11060	6.64565	9.02922	8.02819	**6.36647**	9.68328	7.05427
2	11.15957	7.69535	15.8641	9.86857	7.39351	9.90533	**4.02399**
3	9.90544	5.72177	5.27664	4.76684	5.34809	8.40654	**3.22217**
4	10.22477	7.46902	7.31059	6.87139	7.27843	9.20746	**3.96242**
5	21.00283	10.8517	10.45155	9.98045	10.2265	12.97113	**6.11649**
6	18.87558	5.59715	6.51492	6.26468	5.4149	7.90974	**5.14307**
7	10.55462	7.00617	7.22992	6.26306	6.6755	9.25229	**3.25274**
8	29.43914	9.42024	10.88925	10.07293	8.8916	12.19454	**8.26923**
9	11.42871	4.95249	4.98437	4.55382	4.7792	7.90711	**3.51167**
10	11.57915	5.04072	5.66998	4.9595	4.8884	7.56765	**3.43674**
11	15.83575	6.38388	6.53450	6.44933	6.2189	8.76824	**5.15774**
12	10.85941	4.84798	8.52181	4.2435	4.8247	7.63893	**3.17873**
13	28.37855	8.64134	10.74274	9.93876	**8.3398**	10.43866	10.85466
14	16.15119	12.5304	10.19332	10.28487	12.065	14.90572	**6.01562**
15	12.84651	6.60290	8.39457	5.8504	6.54007	9.19112	**4.56858**
16	13.13128	3.64733	3.95255	3.81453	3.4866	6.21679	**3.32050**
17	11.96246	4.31306	4.58097	4.44911	**4.12538**	7.36074	4.13503
18	18.30394	8.35274	8.38712	7.96032	8.1106	10.23632	**7.05399**
19	18.28229	5.20858	5.51487	5.64718	4.95732	9.56679	**4.71798**
20	13.64456	5.32706	7.82273	5.14884	5.11727	10.44498	**4.46415**
21	17.34255	6.10417	7.10532	6.75874	5.89808	9.2898	**5.88705**
22	14.07647	7.21545	7.31108	6.70476	7.05253	10.0442	**5.49335**
23	8.78402	6.20029	6.19383	5.33330	5.77076	9.5938	**3.10047**
24	21.61794	8.08706	8.65204	8.3929	**7.79311**	11.8098	8.40263
Avg.	15.7290	6.82760	7.797	6.7752	6.5651	9.6046	**5.1809**

Table 4
Comparison of RMSE value with conventional demosaicking algorithms using McMaster Dataset.

Image	BI	GBTF	RI	MLRI	MSG	AP	RD-PSG(Prop)
1	24.5151	24.5270	18.7749	18.9039	23.6360	30.1150	**15.1880**
2	16.3652	10.5043	8.8808	8.9073	10.1604	13.8170	**7.5841**
3	27.9983	12.2109	11.5974	11.2925	11.6974	15.7282	**8.9878**
4	31.4549	12.1676	8.5567	8.8482	11.1859	17.8097	**5.5933**
5	17.6231	16.6487	11.7045	12.1792	16.2944	19.7072	**8.7528**
6	14.1588	16.1170	9.4620	10.0711	15.7232	18.8873	**5.1780**
7	15.2088	4.4466	5.3847	5.0889	**4.2401**	7.0193	6.2168
8	17.5033	6.8005	7.7282	7.2405	6.6311	9.4071	**5.6037**
9	17.2419	12.2653	9.7337	9.8584	11.7643	15.6656	**6.5532**
10	12.9490	9.5419	7.5929	7.2400	9.0260	13.2786	**5.0440**
11	10.4091	8.6768	6.6100	6.0988	8.2503	12.1420	**4.3403**
12	15.5937	7.8943	5.7501	5.8697	7.6469	12.2029	**4.5416**
13	12.4422	6.3022	4.3958	4.5214	6.1611	10.4202	**4.0746**
14	10.6125	6.5133	5.0613	5.0809	6.2392	9.8220	**4.9102**
15	10.7758	7.0904	6.4619	5.6812	6.7442	10.2555	**4.8567**
16	19.0252	18.0982	11.5827	11.7725	17.9561	23.1659	**7.5521**
17	16.8490	24.0710	16.4553	17.6285	23.1908	27.8527	**9.9786**
18	21.5813	10.4083	8.2292	8.3578	10.1053	14.6609	**6.6337**
Avg.	17.3504	11.9046	9.1090	9.14671	11.4807	15.6642	**6.7549**

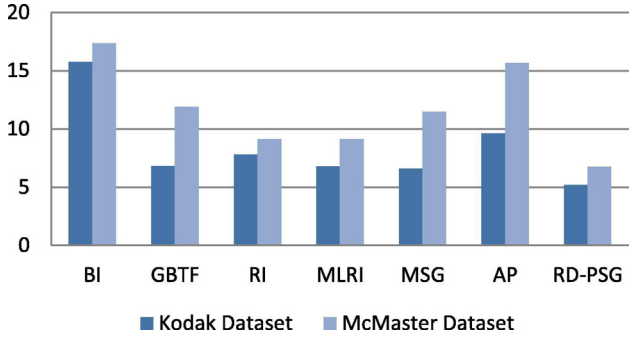

Fig. 8. Comparison of the average RMSE values of the existing and the proposed algorithm.

The tentative estimate for the red and green channel is defined as δ

The cost function of the linear coefficients are identified by Eq. (12) as

$$E(P_{i,j}) = \sum_{a,b\in\omega i,j}\left[\delta Rd_{a,b} - P_{i,j}\delta\left(\hat{G}r^{M}_{a,b}\right)\right]$$
$$E(Q_{i,j}) = \sum_{a,b\in\omega i,j}\left[Rd_{a,b} - P_{i,j}\hat{G}r^{M}_{a,b} - Q_{i,j}\right] \quad (12)$$

where the guide green channel is masked by M .The weight of the residualcost is added to the image. The resulting red channel in each window is different and the demosaicked image is obtained as in Eq. (3) of Section 2.2. A horizontal sparse Laplacian filter [−1 0 2 0–1] is applied to the provisional estimate by guided upsampling. The final stage of obtaining a completely demosaicked red channel is by combining the demosaicked residual image and the assumed provisional estimate. The complete residual demosaicking process is repeated for the blue channel with green as the guided image giving rise to the demosaicked blue channel

Input: Raw or unprocessed input image from Kodak or McMaster dataset

Output: Demosaicked full colour image.

1. *Convert a raw image into a mosaic image by using Bayer colour filter array*
2. *Subsample the three channels red Rd(a,b), green Gr(a,b)and blue Bl(a,b) separately.*
3. *Demosaick the Gr(a,b) with sub-sampled Rd(a,b) using the colour difference polyscale gradients algorithm.*
   - *The horizontal and vertical directional estimates for the red and green channels.*
   - *The difference between the horizontal and vertical directional estimates are* $\hat{\delta}^{Hor}_{Gr,Rd}(a,b)$ and $\hat{\delta}^{\mathrm{Ver}}_{\mathrm{Gr,Rd}}(a,b)$
   - *They are adaptively combined and smoothed and weights are added in four directions.*
   - *Finally the green channel is demosaicked by adding the provisional estimate in Eq. (10).*
4. *Demosaicked green channel acts as the guide through guide upsampling to demosaick the red and blue channels.*
5. *Red and blue channels are demosaicked using residual demosaicking.*
   - *The provisional estimate for a local window is taken to determine the gain component and discriminate capability component.*
   - *Each window has a final output with their cost function estimation obtaining the demosaicked red and blue channels.*
6. *The demosaicked three channels are combined to obtain a full colour image.*

3. Experimental results

The proposed work is compared with the conventional state of the art algorithms. We have analyzed the performance of the proposed work with the Kodak and McM Dataset (Wu, 2011). The test images of the datasets are illustrated in Figs. 5 and 6. The test images are evaluated in MatLab R2014a. The dimension of the images in the dataset is 768x512 in portable network graphics (.png) format. The McMaster dataset consists of 18 images of dimension 500 × 500 in tagged image file (.tiff) format. The conventional demosaicking algorithms involved in analysis are Bilinear Interpolation (BI), Gradient Based Threshold Free algorithm (GBTF) (Pekkucuksen and Altunbasak, 2010), Residual Interpolation (RI) (Kiku et al., 2013), Minimized Laplacian Residual Interpolation (MLRI) (Kiku et al., 2014), Multiscale Gradients (MSG) (Pekkucuksen and Altunbasak, 2013),Alternating Projections(AP) (Lu et al., 2010). The evaluating methods include the Peak Signal to Noise Ratio (PSNR), Root Mean Square Error (RMSE), Structural Similarity Index (SSIM) and Universal Image Quality Index (UIQI). The PSNR value is the difference between the original image and the reconstructed image and the error measures are tested using RMSE, SSIM and UIQI. The effectiveness of the proposed RD-PSG is visualized using the PSNR, RMSE, SSIM and UIQI values respectively. The source codes of the conventional demosaicking algorithms are publicly available in the authors' website.

The proposed PSNR value is comparatively high with regard to the conventional algorithms for Kodak and McMaster dataset. An average of 4.4 db and 4.8 db has exceeded from the conventional demosaicking algorithms for both the datasets.

The detailed analysis of the PSNR value for Kodak and McM dataset is illustrated in Tables 1 and 2 respectively and graphically illustrated in Fig. 7. The overall percentage of improvement in PSNR has increased to 4.4% and 4.8% Kodak and McM dataset than the conventional demosaicking algorithms. An average RMSE value of 3.7 and 5.6 has decreased for Kodak and McMaster datasets and described in detail in Tables 3 and 4 with a graphical representation in Fig. 8. The percentage of reduction in the error values is 3.7% and 5.6% comparatively leading to the reduction of artefacts. Other performance analysis such as Structural Similarity Index (SSIM) and Universal Image Quality Index (UIQI) are also used to test the performance of the proposed work. Tables 5 and 6 illustrates the SSIM performance measures pictured in Fig. 9, Tables 7 and 8 describes the UIQI values in detail of the state of art algorithms and of the proposed work for Kodak and McMaster dataset which is pictured in Fig. 10. The proposed work is effective in 83.3% of the images in Kodak dataset and 94.4% images in McMaster

Table 5
Comparison of SSIM value with conventional demosaicking algorithms using Kodak Dataset.

Image	BI	GBTF	RI	MLRI	MSG	AP	RD-PSG(Prop)
1	0.8377	0.9850	0.9699	0.9764	**0.9863**	0.9701	0.9834
2	0.9852	0.9934	0.9901	0.9897	0.9941	0.9890	**0.9985**
3	0.9573	0.9914	0.9919	0.9921	0.9917	0.9734	**0.9949**
4	0.9705	0.9902	0.9912	0.9910	0.9907	0.9827	**0.9966**
5	0.8486	0.9761	0.9736	0.9757	0.9786	0.9582	**0.9908**
6	0.8899	0.9860	0.9821	0.9836	0.9864	0.9743	**0.9916**
7	0.9341	0.9889	0.9888	0.9902	0.9898	0.9764	**0.9959**
8	0.8223	0.9760	0.9702	0.9727	0.9776	0.9590	**0.9785**
9	0.8982	0.9813	0.9825	0.9823	0.9815	0.9584	**0.9879**
10	0.8934	0.9844	0.9840	0.9854	0.9852	0.9624	**0.9863**
11	0.8943	0.9745	0.9759	0.9750	0.9752	0.9549	**0.9786**
12	0.9614	0.9929	0.9887	0.9936	0.9932	0.9852	**0.9951**
13	0.8584	0.9800	0.9720	0.9757	**0.9814**	0.9694	0.9767
14	0.8658	0.9740	0.9735	0.9753	0.9757	0.9551	**0.9857**
15	0.9556	0.9869	0.9857	0.9869	0.9876	0.9767	**0.9877**
16	0.8442	0.9840	0.9811	0.9812	0.9849	0.9553	**0.9887**
17	0.8940	0.9876	0.9877	0.9879	**0.9882**	0.9698	0.9786
18	0.8896	0.9691	0.9702	0.9719	0.9702	0.9575	**0.9720**
19	0.8976	0.9852	0.9865	0.9864	0.9857	0.9529	**0.9877**
20	0.9052	0.9613	0.9605	0.9643	0.9577	0.9164	0.9617
21	0.9008	0.9850	0.9834	0.9846	0.9858	0.9679	**0.9866**
22	0.9097	0.9742	0.9762	0.9778	0.9745	0.9452	**0.9823**
23	0.9627	0.9912	0.9917	0.9936	0.9922	0.9727	**0.9942**
24	0.8503	0.9712	0.9696	0.9795	**0.9796**	0.9412	0.9790
Avg.	0.901117	0.982075	0.980292	0.9822	0.983075	0.963504	**0.985792**

Table 6
Comparison of SSIM value with conventional demosaicking algorithms using McMaster Dataset.

Image	BI	GBTF	RI	MLRI	MSG	AP	RD-PSG(Prop)
1	0.9358	0.9465	0.9655	0.9646	0.9493	0.9262	**0.9691**
2	0.9361	0.9659	0.9724	0.9727	0.9675	0.9488	**0.9734**
3	0.8374	0.9646	0.9684	0.9699	0.9649	0.9274	**0.9727**
4	0.8183	0.9680	0.9778	0.9766	0.9650	0.9050	**0.9837**
5	0.9245	0.9449	0.9677	0.9650	0.9459	0.9176	**0.9727**
6	0.9179	0.9012	0.9544	0.9492	0.9033	0.8738	**0.9689**
7	0.8371	0.9753	0.9694	0.9712	**0.9758**	0.9558	0.9447
8	0.8755	0.9517	0.9568	0.9564	0.9527	0.9323	**0.9555**
9	0.9561	0.9772	0.9854	0.9853	0.9789	0.9648	**0.9897**
10	0.9697	0.9819	0.9864	0.9869	0.9832	0.9704	**0.9875**
11	0.9717	0.9752	0.9866	0.9877	0.9766	0.9641	**0.9892**
12	0.9725	0.9946	0.9970	0.9967	0.9949	0.9844	**0.9974**
13	0.9759	0.9942	0.9983	0.9970	0.9945	0.9822	**0.9984**
14	0.9718	0.9860	0.9892	0.9901	0.9871	0.9736	**0.9912**
15	0.9732	0.9827	0.9856	0.9870	0.9840	0.9725	**0.9873**
16	0.9520	0.9630	0.9827	0.9826	0.9631	0.9517	**0.9907**
17	0.9555	0.9221	0.9628	0.9590	0.9270	0.9046	**0.9829**
18	0.9386	0.9734	0.9827	0.9819	0.9737	0.9614	**0.9852**
Avg.	0.928867	0.964911	0.977117	0.976656	0.965967	0.945367	**0.980011**

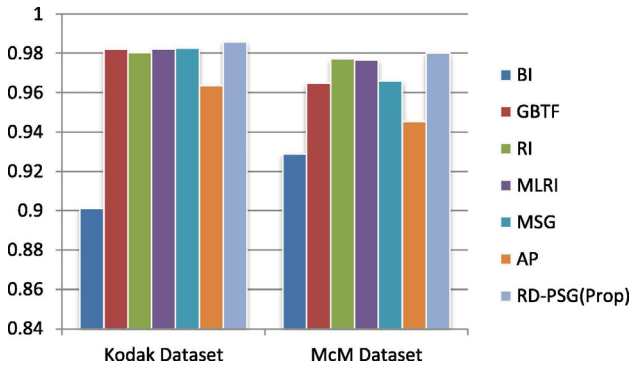

Fig. 9. Comparison of the average SSIM values of the existing and the proposed algorithm.

dataset. Certain images in Kodak and McMaster dataset have low intensity value which moderates the performance of the proposed work and can be overcome by increasing the saturation of the images. The gradients at half the scale help to obtain good results in the images of high intensity values. The time complexity of the algorithms is diagrammatically represented in Fig. 11 with an increase in the amount of time than a few algorithms and a decrease in the time complexity from a few but produces drastic performance than the conventional demosaicking algorithms. The demosaicked performance is comparatively high and has proved authentic among the existing state of art algorithms. The proposed work effectively demosaics the image of both the Kodak and McMaster dataset. The Laplacian value is minimized as it reduces the artefacts of the image. The demosaicking approach outperforms the existing demosaicking algorithms.

Table 7
Comparison of UIQI value with conventional demosaicking algorithms using Kodak Dataset.

Image	BI	GBTF	RI	MLRI	MSG	AP	RD-PSG(Prop)
1	0.69986	0.97106	0.95304	0.96123	**0.97240**	0.94712	0.96247
2	0.68548	0.86759	0.89729	0.89463	0.86545	0.77837	**0.91438**
3	0.76359	0.87393	0.89393	0.90296	0.88175	0.84147	**0.90853**
4	0.80920	0.95037	0.95270	0.95469	0.95024	0.92801	**0.95605**
5	0.79770	0.95707	0.95881	0.96337	0.96089	0.94491	**0.97772**
6	0.67672	0.94099	0.93440	0.93950	0.94371	0.92492	**0.94808**
7	0.83874	0.92779	0.93782	0.93817	0.93072	0.90597	**0.94787**
8	0.76187	0.96918	0.96228	0.96409	0.97127	0.95485	**0.97221**
9	0.75978	0.85512	0.87804	0.87034	0.85643	0.82756	0.87813
10	0.77221	0.92734	0.93599	0.91755	0.92971	0.90798	0.91770
11	0.72443	0.93496	0.93259	0.93572	0.93669	0.90952	**0.94119**
12	0.73145	0.91978	0.91678	0.92395	0.92171	0.89587	**0.92687**
13	0.70662	0.94078	0.92691	0.95170	**0.95475**	0.93705	0.95166
14	0.80697	0.92044	0.94388	0.95029	0.92558	0.90412	**0.96234**
15	0.79463	0.89399	0.91668	0.91783	0.89689	0.86611	0.91786
16	0.74037	0.94342	0.94589	0.93953	0.94608	0.92286	0.94099
17	0.84744	0.95883	0.96321	0.96381	**0.96999**	0.94734	0.94419
18	0.73335	0.90995	0.91088	0.92538	0.91378	0.89931	**0.93968**
19	0.73216	0.93029	0.93453	0.93646	0.93229	0.90607	**0.93673**
20	0.76024	0.83433	0.78861	0.77630	0.83656	0.79706	**0.85331**
21	0.72910	0.83999	0.85887	0.85006	0.84134	0.81664	**0.88141**
22	0.74260	0.89066	0.89611	0.90369	0.89325	0.86795	**0.92299**
23	0.89621	0.92635	0.94718	0.94396	0.93245	0.89043	**0.94441**
24	0.77875	0.94743	0.94323	0.94733	**0.95014**	0.93022	0.93700
Avg.	0.762061	0.917985	0.922069	0.923856	0.92142	0.893821	**0.932657**

Table 8
Comparison of UIQI value with conventional demosaicking algorithms using McMaster Dataset.

Image	BI	GBTF	RI	MLRI	MSG	AP	RD-PSG(Prop)
1	0.79832	0.73778	0.82893	0.82214	0.74558	0.70567	**0.83195**
2	0.83341	0.85289	0.90155	0.89766	0.85798	0.82071	**0.90309**
3	0.77016	0.90354	0.91993	0.91084	0.90696	0.88366	**0.91648**
4	0.83525	0.94822	0.96230	0.96148	0.95014	0.92093	**0.96076**
5	0.86250	0.89300	0.92548	0.92050	0.89634	0.87045	**0.92587**
6	0.85934	0.76197	0.90510	0.89655	0.77283	0.73795	**0.91802**
7	0.80897	0.92100	0.93212	0.92623	**0.93329**	0.91090	0.86946
8	0.73910	0.77250	0.82058	0.81093	0.77358	0.75377	**0.82211**
9	0.74254	0.73326	0.80425	0.79263	0.73963	0.71223	**0.80749**
10	0.79521	0.78340	0.86078	0.85261	0.79129	0.75394	**0.88188**
11	0.79641	0.55135	0.75756	0.74383	0.56114	0.52515	**0.80925**
12	0.67362	0.72850	0.76899	0.76148	0.73167	0.70234	**0.78446**
13	0.62755	0.67511	0.69381	0.68897	0.67763	0.64753	**0.69892**
14	0.86225	0.85381	0.88943	0.89398	0.85861	0.83003	**0.89469**
15	0.75405	0.69873	0.80024	0.77928	0.70780	0.66895	**0.81709**
16	0.78799	0.60409	0.86246	0.85450	0.61133	0.58341	**0.90005**
17	0.85580	0.71280	0.87716	0.86719	0.72770	0.68205	**0.89866**
18	0.78187	0.85221	0.92220	0.92062	0.85379	0.83117	**0.92415**
Avg.	0.788019	0.776898	0.857382	0.850079	0.783183	0.752269	**0.864688**

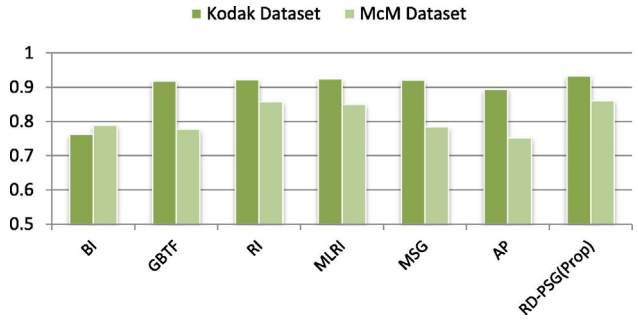

Fig. 10. Comparison of the average UIQI values of the conventional and the proposed algorithm.

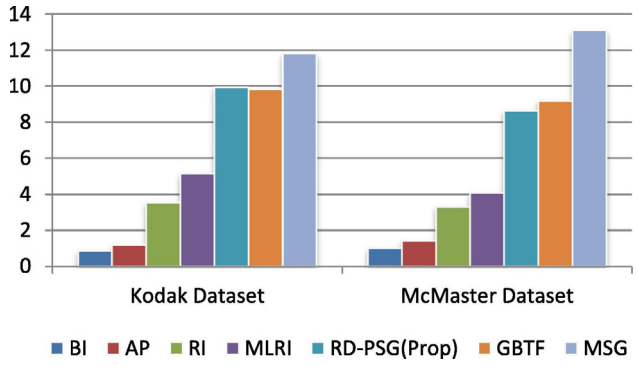

Fig. 11. Comparison of the average time complexity of the conventional and proposed algorithm.

4. Conclusion

In this paper, the polyscale gradients residual demosaicking algorithm is proposed. The demosaicking is implemented with gradients at different scales to obtain the best possible outcome for green and in the residual province for the blue and red colour channels. The proposed work has experimentally proved the effectiveness for both the Kodak and the McMaster dataset. The accuracy is improved and the error measure is reduced drastically due to the minimization of the Laplacian energy of the colour channels. The work can be extended further by concentrating highly on the error measures and reducing the artefacts of the demosaicked image.

References

Bayer, B.E., 1976. Color Imaging Array. U S Pat. 350–317.
Buades, A., Coll, B., Morel, J.M., Sbert, C., Buades, A., Coll, B., Morel, J., Sbert, C., 2009. Self-similarity driven color demosaicking. IEEE Trans. Image Process. 18, 1192–1202.
Chung, K.H., Chan, Y.H., 2006. Color demosaicing using variance of color differences. IEEE Trans. Image Process. 15, 2944–2955. https://doi.org/10.1109/TIP.2006.877521.
Chung, K.L., Yang, W.J., Yan, W.M., Wang, C.C., 2008. Demosaicing of color filter array captured images using gradient edge detection masks and adaptive heterogeneity-projection. IEEE Trans. Image Process. 17, 2356–2367. https://doi.org/10.1109/TIP.2008.2005561.
Duran, J., Buades, A., 2014. Self-Similarity and Spectral Correlation Adaptive Algorithm for Color Demosaicking. IEEE Trans. Image Process. 23, 4031–4040.
Gunturk, B.K., Glotzbach, J., Altunbasak, Y., Schafer, R.W., Mersereau, R.M., 2005. Demosaicking: color filter array interpolation. IEEE Signal Process. Mag. 22, 44–54. https://doi.org/10.1109/MSP.2005.1407714.
He, K., Sun, J., Tang, X., 2013. Guided image filtering. IEEE Trans. Pattern Anal. Mach. Intell. 35, 1397–1409. https://doi.org/10.1109/TPAMI.2012.213.
Horé, A., Ziou, D., 2010. An edge-sensing universal demosaicing algorithm. Lect. Notes Comput. Sci. (including Subser. Lect. Notes Artif. Intell. Lect. Notes Bioinformatics) 6474 LNCS, 197–208. doi:10.1007/978-3-642-17688-3_20
Kang, M.G., Oh, H.M., Kim, C.W., Han, Y.S., 2010. Edge adaptive color demosaicking based on the spatial correlation of the bayer color difference. Eurasip J. Image Video Process. 2010, 1–14. https://doi.org/10.1155/2010/874364.
Kiku, D., Monno, Y., Tanaka, M., Okutomi, M., 2016. Beyond Color Difference: Residual Interpolation for Color Image Demosaicking. IEEE Trans. Image Process. 25, 1288–1300. https://doi.org/10.1109/TIP.2016.2518082.
Kiku, D., Monno, Y., Tanaka, M., Okutomi, M., 2014. Minimized-Laplacian residual interpolation for color image demosaicking. Proc. SPIE-IS&T Electron. Imaging 9023. https://doi.org/10.1117/12.2038425.
Kiku, D., Monno, Y., Tanaka, M., Okutomi, M., 2013. Residual Interpolation for Color Image Demosaicking. Proc. - Int. Conf. Image Process. ICIP 2304–2308. doi:10.1109/TIP.2016.2518082
Kim, Y., Jeong, J., 2016. Four-Direction Residual Interpolation for Demosaicking. IEEE Trans. Circuits Syst. Video Technol. 26, 881–890. https://doi.org/10.1109/TCSVT.2015.2428552.
Li, N., Li, J.S.J., Randhawa, S., 2017. Color Filter Array Demosaicking Based on the Distribution of Directional Color Differences. IEEE Signal Process. Lett. 24, 604–608. https://doi.org/10.1109/LSP.2017.2658667.
Lu, Y.M., Karzand, M., Vetterli, M., 2010. Demosaicking by alternating projections: theory and fast one-step implementation. IEEE Trans. Image Process. 19, 2085–2098. https://doi.org/10.1109/TIP.2010.2045710.
Monno, Y., Kiku, D., Tanaka, M., Okutomi, M., 2015. Adaptive Residual Interpolation for Color Image Demosaicking. Proc. - Int. Conf. Image Process ICIP.
Ousguine, S., Essannouni, F., Essannouni, L., Abbad, M., Aboutajdine, D., 2016. A New Image Interpolation Using Laplacian Operator. Int. Symp. Ubiquituous Newtworking 403–413. https://doi.org/10.1007/978-981-287-990-5.
Pekkucuksen, I., Altunbasak, Y., 2013. Multiscale gradients-based color filter array interpolation. IEEE Trans. Image Process. 22, 157–165. https://doi.org/10.1109/TIP.2012.2210726.

Pekkucuksen, I., Altunbasak, Y., 2010. Gradient based threshold free color filter array interpolation. Proc. - Int. Conf. Image Process. ICIP 137–140. doi:10.1109/ICIP.2010.5654327

Wu, J., Anisetti, M., Wu, W., Damiani, E., Jeon, G., 2016. Bayer demosaicking with polynomial interpolation. IEEE Trans. Image Process. 25, 5369–5382. https://doi.org/10.1109/TIP.2016.2604489.

Wu, X., 2011. Color demosaicking by local directional interpolation and nonlocal adaptive thresholding. J. Electron. Imaging 20, 23016. https://doi.org/10.1117/1.3600632.

Ye, W., Ma, K.K., 2015. Color Image Demosaicing Using Iterative Residual Interpolation. IEEE Trans. Image Process. 24, 5879–5891. https://doi.org/10.1109/TIP.2015.2482899.

Zhang, C., Li, Y., Wang, J., Hao, P., 2016. Universal demosaicking of color filter arrays. IEEE Trans. Image Process. 25, 5173–5186. https://doi.org/10.1109/TIP.2016.2601266.

Zhang, F., Wu, X., Yang, X., Zhang, W., Zhang, L., 2009. Robust color demosaicking with adaptation to varying spectral correlations. IEEE Trans. Image Process. 18, 2706–2717. https://doi.org/10.1109/TIP.2009.2029987.

Zhang, L., Wu, X., Member, S., 2005. Color Demosaicking Via Directional Linear Minimum Mean Square Error Estimation. IEEE Trans. Image Process. 14, 2167–2178.

Kodak Dataset - http://r0k.us/graphics/kodak/